DOCKET NO: 209663US0PCT

IN THE UNITED STATES PATENT & TRADEMARK OFFICE

IN RE APPLICATION OF	:
YUKO TACHIBANA, ET AL.	: EXAMINER: PIZIALI, A. T.
SERIAL NO: 09/857,209	:
FILED: JUNE 22, 2001	: GROUP ART UNIT: 1771
FOR: LAMINATE AND ITS PRODUCTION METHOD	:

DECLARATION UNDER 37 C.F.R. § 1.132

COMMISSIONER FOR PATENTS
ALEXANDRIA, VIRGINIA 22313

SIR:

I, Yuko TACHIBANA, a citizen of Japan, hereby declare and state that:

1. I am one of the inventors of the above-identified application.

2. I have been employed by Asahi Glass, Ltd. ~~between~~ Since 1990 ~~and 2000. During this time~~ Between 1990 and 2000, my activities have included the research and development of film formation technologies by sputtering methods.

Yuko Tachibana Y.T.

3. First I will discuss the present invention, which relates to titanium oxide/metal laminates. Then I will present comparative data obtained using zinc oxide/metal laminates.

4. The above-identified application is the solution for the peculiar problem that the absorption at the silver/dielectric-material interfaces occurs in the silver/dielectric-material multilayers, in the case that the dielectric material is titanium oxide which has high refractive index. My co-inventor and I think this problem is caused by the phenomenon which depends on the dielectric constant of the dielectric material, which means the refractive index in the case of the transparent material.

We think it can be thought this absorption occurs by the phenomenon that the surface plasmons of silver are excited in light irradiation, which is mentioned in the specification at page 9, lines 4-12. The energy that the surface plasmons of silver are excited depends on the dielectric constant of the surroundings, in this case the dielectric material. In detail, the absorbed energy decreases with the increase of the dielectric constant of the dielectric material, which means the increase of the refractive index in the case of the transparent material. This absorbed energy reaches to the visible region in the case of titanium oxide, as a result of the energy shift from UV region. We think this is the reason why the above peculiar problem occurs in the case that the dielectric material is titanium oxide.

In general, two reasons have been well known why the absorption at the silver/dielectric-material interfaces occurs. One reason is due to the absorption caused by the oxidation of silver at the interface when the dielectric material is deposited on the silver layer. The other reason is due to the absorption caused by that one part of the protective metal layer is not fully oxidized and remains as absorption layer when the dielectric material is deposited on the protective layer, in the case the metal layer is used as the protective layer of the silver from oxidation during the deposition of the dielectric material.

In the former case, the measurement of electrical resistance is well known to the effective measure to verify whether the silver is oxidized or not, because silver has very low resistance and the resistance increases very sensitively in the case the silver is oxidized.

The electrical resistance in the comparative examples 1, 6, 7, 9, 10, 11, which did not have the interlayers and the protective layers, were very low and same as those of the examples which had the interlayers. These results show the silver was not oxidized in the comparative examples which did not have the interlayers and the protective layers, when the titanium oxide was deposited on the silver layer. These results also show the effect of the interlayers is not to protect the silver from oxidation.

It has been unexpected that the absorption occurs at the interlayer between the silver and the dielectric material, in spite that the silver is not oxidized at the interface and the protective metal layer is not applied.

My co-inventor and I found that the absorption at the silver/titanium interfaces occurs in the silver/titanium multilayers in spite that the silver is not oxidized. We think it can be thought this absorption occurs by the phenomenon that the surface plasmons of silver are excited in light irradiation and this absorbed energy, which depends on the dielectric constant of the dielectric material, reaches to the visible region in the case of titanium oxide, as a result of the energy shift from UV region. We could find the solution of this problem by understanding this mechanism.

Furthermore, we will add to explain the reason why the silver was not oxidized in the comparative examples which do not have the interlayers and the protective layers, when the titanium oxide was deposited directly on the silver layer. We used the titanium oxide target and very small amount of oxygen gas (the amount of oxygen is only 2% of gas) for the deposition of titanium oxide layer in the examples and the comparative examples. In this case, the oxygen which contain in the titanium oxide layer mainly come from the sputter target. The species which eject from the sputter target are electrically neutral and do not accelerate in the electric field in sputter system, therefore, reach to the substrate by having lower kinetic energy. On the other hand, the oxygen ions which come from oxygen gas have electrical charges and are accelerated in the electric field in sputter system, therefore, reach to the substrate by having higher kinetic energy. Therefore, oxygen which come from the sputter target do not oxidize the silver and the oxygen ions which come from oxygen gas contribute to oxidize the silver. By having used only 2% oxygen in sputter gas, the silver was not oxidized in our comparative examples, in spite that the titanium oxide was deposited directly on the silver layer without the interlayers and the protective layers.

We presented the research results concerning the above-identified application at several international technical conferences including one of the meetings of Optical Society of America, and published the several technical journals as listed below:

- 4th International Conference of Coatings on Glass (2002);
- 5th International Symposium of Sputtering & plasma Processes (2003);
- Optical Interference Coatings 9th Topical Meeting; (one of the technical meetings of Optical Society of America, 2004);
- Y. Tachibana, K. Kusunoki, T. Watanabe, K. Hashimoto, H. Ohsaki, Thin Solid Films, 442,212 (2003);
- Y. Tachibana, K. Kusunoki, H. Ohsaki, Vacuum, 74, 555 (2004).

In addition, we also presented the research result concerning to the deposition of titanium oxide using the oxide target as listed below:

- Society of Vacuum Coaters 42nd Annual Technical Conference (1999);
- 4th International Symposium of Sputtering & Plasma Processes (1999);
- H. Ohsaki, Y. Tachibana, A. Hayashi, A. Mitsui and Y Hayashi, Thin Solid Films, 351, 57 (1999);
- Y. Tachibana, H. Ohsaki, A. Hayashi. A. Mitsui and Y. Hayashi, Vacuum, 59, 836 (2000);
- H. Ohsaki, Y. Tachibana, A. Mitsui, T. Kamiyama and Y. Hayashi, Thin Solid Films, 392,169 (2001).

For the Examiner's convenience, attached are copies of

- Y. Tachibana, K. Kusunoki, T. Watanabe, K. Hashimoto, H. Ohsaki, Thin Solid Films, 442,212 (2003); and
- H. Ohsaki, Y. Tachibana, A. Hayashi, A. Mitsui and Y Hayashi, Thin Solid Films, 351, 57 (1999).

5. Having discussed the present invention relating to titanium oxide/metal laminates, I will now present comparative data obtained using zinc oxide/metal laminates.

6. The following experiments were carried out by me or under my direct supervision and control.

7. Object

I aimed to substantiate the inventive step of the above-identified application by showing that no change of a visible light transmittance is observed in a laminate obtained by using zinc oxide instead of titanium oxide for a dielectric layer in this application.

8. Method of experiments and results of experiments

(1) Experiments repeating Examples 48, 51, 52 and 54 and Comparative Example 9 in the above-identified application provided that zinc oxide was used instead of titanium oxide.

a. Sample 1

① Formation of a zinc oxide layer

Using a zinc oxide target (area: 432 mm x 127 mm), a zinc oxide layer having a thickness of 36 nm was formed on the surface of a soda lime glass, with an application of electric power of 2 kw in an argon gas atmosphere.

② Formation of a Ag-Pd layer

On this zinc oxide layer, a silver layer containing 1 atomic% of palladium with a thickness of 12 nm was formed by using a silver target (area: 432 mm x 127 mm) containing 1 atomic% of palladium in an argon gas atmosphere by applying an electric power of 0.3 kw.

The operations ① and ② were similarly repeated to obtain a laminate (Sample 1) having the layer structure as indicated in Table 1 below.

b. Sample 2

① Formation of a zinc oxide layer

A zinc oxide layer was formed in a thickness of 36 nm on a soda lime glass by similarly conducting the operation ① of Sample 1.

② Formation of a SiN layer

On this zinc oxide layer, a SiN layer having a thickness of 1 nm was formed by using a Si target (area: 432 mm x 127 mm) in an argon gas atmosphere containing 30 vol% of nitrogen by applying an electric power of 1 kw.

③ Formation of a Ag-Pd layer

On the obtained SiN layer, a silver layer containing 12 atomic% of palladium was formed in a thickness of 12 nm by conducting the operation ② of Sample 1 similarly.

The above operations ① to ③ were similarly repeated to obtain a laminate (Sample 2) having the layer structure as indicated in Table 1 below.

c. Sample 3

① Formation of a zinc oxide layer

A zinc oxide layer was formed in a thickness of 36 nm on a soda lime glass by similarly conducting the operation ① of Sample 1.

② Formation of a SiN layer

On this zinc oxide layer, a SiN layer was formed in a thickness of 3 nm by conducting the operation ② of Sample 2 similarly.

③ Formation of a Ag-Pd layer

On the obtained SiN layer, a silver layer containing 1 atomic% of palladium was formed in a thickness of 12 nm by conducting the operation ② of Sample 1 similarly.

The operations ① to ③ were similarly repeated to obtain a laminate (Sample 3) having the layer structure as indicated in Table 1 below.

d. Sample 4

① Formation of a zinc oxide layer

A zinc oxide layer was formed in a thickness of 36 nm on a soda lime glass by conducting the operation ① of Sample 1 similarly.

② Formation of a SiN layer

On this zinc oxide layer, a SiN layer was formed in a thickness of 5 nm by conducting the operation ② of sample 2 similarly.

③ Formation of a Ag-Pd layer

On the obtained SiN layer, a silver layer containing 1 atomic% of palladium was formed in a thickness of 12 nm by conducting the operation ③ of Sample 1 similarly.

The operations ① to ③ were similarly repeated to obtain a laminate (Sample 4) having the layer structure as indicated in Table 1 below.

(2) Samples obtained

① Sample 1: A laminate having the following structure consisting of five ZnO layers and four Ag layers.

Substrate/ZnO/Ag/ZnO/Ag/ZnO/Ag/ZnO/Ag/ZnO

② Sample 2: In Sample 1, SiN layers having a thickness of 1 nm were formed above and below all the Ag layers.

③ Sample 3: In Sample 1, SiN layers having a thickness of 3 nm were formed above and below all the Ag layers.

④ Sample 4: in Sample 1, SiN layers having a thickness of 5 nm were formed above and below all the Ag layers.

(3) Results of evaluation

Using the obtained laminates, the following evaluations were conducted.

① visible light transmittance (%)

② Visible light reflectance (%)

③ Sheet resistance (Ω/□)

Table 1

Results of evaluation of laminates when zinc oxide was used

	Sample 1	Sample 2	Sample 3	Sample 4
17. Zinc oxide layer (5)	36	36	36	36
16. SiN layer	-	1	3	5
15. Ag-1 at% Pd layer	12	12	12	12
14. SiN layer	-	1	3	5
13. Zinc oxide layer (4)	68	68	68	68
12. SiN layer	-	1	3	5
11. Ag-1 at% Pd layer	15	15	15	15
10. SiN layer	-	1	3	5
9. Zinc oxide layer (3)	65	65	65	65
8. SiN layer	-	1	3	5
7. Ag-1 at% Pd layer	15	15	15	15
6. SiN layer	-	1	3	5
5. Zinc oxide layer (2)	68	68	68	68
4. SiN layer	-	1	3	5
3. Ag-1 at% Pd layer	12	12	12	12
2. SiN layer	-	1	3	5
1. Zinc oxide layer (1)	36	36	36	36
Substrate				
Visible light transmittance (%)	55.5	55.5	55.5	55.5
Visible light reflectance (%)	2	2	2	2
Sheet resistance (Ω/□)	1.5	1.5	1.5	1.5

*Note: The unit of the thickness of each layer in the laminate is nm.

9. Conclusion

It was confirmed from the results of Table 1 that when zinc oxide was used for a dielectric layer, no change of the visible light transmittance was observed in the obtained laminates, unlike the case when a titanium oxide layer was used as in the present invention.

10. I hereby declare that all statements made herein of my own knowledge are true and that all statements made on information and belief are believed to be true; and further that these statements were made with the knowledge that willful false statements and the like so made are punishable by fine or imprisonment, or both, under Section 1001 of Title 18 of the United States Code and that such willful false statements may jeopardize the validity of this application or any patent issuing thereon.

11. Further declarant saith not.

Date: March 18, 2005 Yuko Tachibana

Yuko TACHIBANA

Attached:
Thin Solid Films, 442, 212 (2003)
Thin Solid Films, 351, 57 (1999)

Available online at www.sciencedirect.com
SCIENCE DIRECT®
Thin Solid Films 442 (2003) 212–216
thin solid films
www.elsevier.com/locate/tsf

Optical properties of multilayers composed of silver and dielectric materials

Yuko Tachibana[a,*], Kouji Kusunoki[b], Toshiya Watanabe[b], Kazuhito Hashimoto[b], Hisashi Ohsaki[b]

[a]Research Center, Asahi Glass Co., Ltd, Hazawa-cho, Kanagawa-ku, Yokohama 21-8755, Japan
[b]Research Center for Advanced Science and Technology, The University of Tokyo, Komaba, Meguro-ku, Tokyo 153-8904, Japan

Abstract

We investigated the optical properties of the silver/dielectric-material multilayers and found that the absorption exists at the silver/dielectric-material interfaces. The absorption was assigned to the absorption of surface plasmon by spectral and ellipsometric analysis and X-ray photoelectron spectroscopy (XPS). The absorption was detected as the difference between the measured transmittance and the calculated one with using the optical constants of constituent layers. The absorption increases with the number of the silver/dielectric-material interfaces and with the dielectric constant of the dielectric materials. By considering the absorbing layer at the silver/dielectric-material interface, the ellipsometric analysis gives a good fit of the optical constants and thicknesses of constituent layers and the measured transmittance agrees well with the calculated one using the ellipsometrically obtained results. XPS analysis showed that the resonant energy of the surface plasmon, excited inside the silver layer but in the vicinity of the silver/dielectric-material interface, decreases with the increase of the thickness of the dielectric material and with the increase of the dielectric constant of the dielectric material. This energy shift of the surface plasmon is consistent with the optical absorption measured.

Keywords: Silver; Dielectric constant; Absorption; Plasmons

1. Introduction

Silver film has a low refractive index approximately 0.1 in visible wavelength region. These kind of optical characteristics enable to design the bandpass filter with a layer construction of a sandwich of silver layer with two dielectric-material layers or its reiteration [1].

Such silver/dielectric-material multilayers have been applied to the low emissivity coatings and recently extended the application to the electromagnetic interference shielding filter for the plasma display panel, featuring the silver's lowest electric resistance [2].

When the optical devices including a basic layer construction of silver/dielectric material are designed, the transmission of the practically prepared device is lower than the calculated one using the optical constants of constituent layers, which is obtained from each single layer. The difference of the transmittance increases on the optical device with the larger number of reiteration of dielectric material/silver/dielectric material, which has a sharper band edge. Also, the difference increases when using a dielectric material with a large dielectric constant; the bandpass filter has a wider optical window in wavelength scale.

In this paper, we will discuss the mechanism of this abnormal absorption and also give ways to increase the transmittance based on the experimental and analytical results.

2. Experimental

We used in-line type planar magnetron sputter coaters (Nisshin Seiki Co., JVS-S0-3 and BOC Coating Technology, ILS-1600) having a deposition chamber with load lock and over run chambers on both ends. The deposition chamber is divided into three chambers with one cathode in each one. The sputter gas is introduced to each deposition chamber and evacuated through the end chambers with two diffusion pumps. The DC power supply is a switching regulator (Advanced Energy Ind., MDX). While the silver layers were deposited by the Ar sputtering of the silver target, dielectric materials were deposited by using the ceramics targets and a mixed sputter gas of a few percent of O_2 diluted with

*Corresponding author.

0040-6090/03/$ - see front matter © 2003 Elsevier B.V. All rights reserved.
doi:10.1016/S0040-6090(03)00984-2

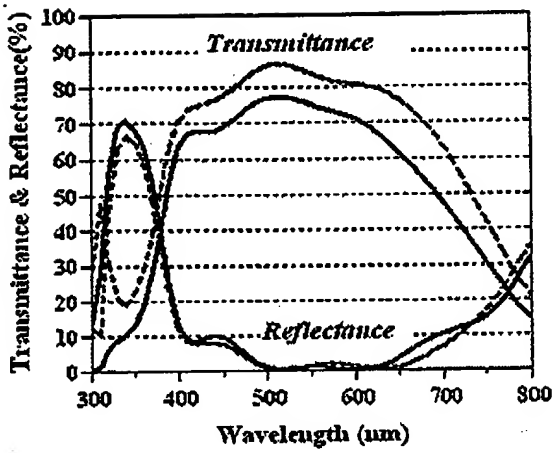

Fig. 1. Spectral transmittance and reflectance of the Ag/SiN_x multi-stack with four Ag layers. Solid and dashed lines represent experimental and calculated ones, respectively. The layer construction is as follows: SiN_x (51 nm)/Ag(12 nm)/SiN_x(89 nm)/Ag(12 nm)/SiN_x(75 nm)/Ag(12 nm)/SiN_x(75 nm)/Ag(12 nm)/SiN_x(36 nm)/glass.

Ar in order to avoid the oxygen damage on silver layers [3].

The thickness of the films was measured using a stylus-type surface tracer (Rank Taylor Hobson, Talystep). The thickness of each constituent layer of multi-stacks is adjusted by using the obtained thicknesses of the monolayer that was deposited at the same deposition condition. The electrical resistance of the films was measured by a non-contact conductance monitor (DELCOM Instruments, Inc., MODEL 717B). Spectral transmittance and reflectance were measured by using a spectrometer (JASCO, ART-25GT). The optical constants of the films were analyzed by ellipsometry using a spectroscopic ellipsometer (J.A. Woolam Co., Inc., VASE). The surface related excitation in silver layer was analyzed using an X-ray photoelectron spectroscope (Physical Electronics, Quantum 2000).

3. Results and discussion

3.1. Spectral analysis of the multilayers of Ag/dielectric material

The Ag/SiN_x multilayer stacks including various numbers of silver layers were prepared and the transmittance was measured. The single layers of Ag and SiN_x were also prepared and their optical constants were analyzed by ellipsometry by using an appropriate n-k model for each material: Caucy polynomials for SiN_x, parametric semiconductor model for TiO_2 and ZnO and Lorentz oscillator model for Ag. We calculated the transmittance of the Ag/SiN_x multilayer stacks by use of the optical constants measured. The Ag/TiO_2 multilayer stacks were also prepared and the measured and calculated transmittances were compared.

Fig. 1 shows the measured and calculated spectral transmittance and reflectance of a Ag/SiN_x multi-stack with four Ag layers and Fig. 2 gives the difference between the measured visible transmittance and the calculated one. The difference increases with the increase of the number of silver layers, as presented in Fig. 2. It is obvious that the Ag/TiO_2 multilayer stacks have a larger difference than the Ag/SiN_x multilayer stacks.

In order to make clear whether this absorption comes from the bulk silver or silver/dielectric-material interface, we inserted 1.0-nm-thick SiN_x interlayer(s) between Ag and TiO_2 in the Ag/TiO_2 multilayer stacks. Fig. 3 shows the visible transmittance and reflectance of Ag/TiO_2 multilayer stacks with and without SiN_x insert layer(s). The results are quite simple; the transmittance increases almost the same percent by each insertion; the increment is independent of the position of insertion. We obtained the same results in the ZnO interlayer case. It is noted that the increment of trans-

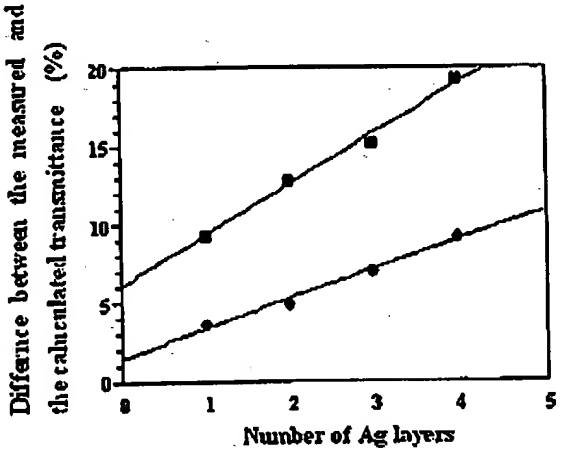

Fig. 2. The difference between the measured and calculated transmittance of the Ag/TiO_2 and the Ag/SiN_x multilayer stacks. Squares represent the difference in the Ag/TiO_2 stacks and circles represent the difference in the Ag/SiN_x stacks. The layer constructions are as follows: (1) TiO_2 (33 nm)/Ag (12 nm)/TiO_2 (33 mm)/glass, SiN_x (40 nm)/Ag (12 nm)/SiN_x (40 nm)/glass; (2) TiO_2 (38 nm)/Ag (12 nm)/TiO_2 (74 mm)/Ag (12 nm)/TiO_2 (42 nm)/glass, SiN_x (45 nm)/Ag (12 nm)/SiN_x (89 mm)/Ag (12 nm)/SiN_x (51 nm)/glass; (3) TiO_2 (42 nm)/Ag (12 nm)/TiO_2 (74 nm)/Ag (12 nm)/TiO_2 (63 nm)/Ag (12 nm)/TiO_2 (30 nm)/glass, SiN_x (51 nm)/Ag (12 nm)/SiN_x (89 nm)/Ag (12 nm)/SiN_x (75 nm)/Ag (12 nm)/SiN_x (36 nm)/glass; (4) TiO_2 (42 nm)/Ag (12 nm)/TiO_2 (74 nm)/Ag (12 nm)/TiO_2 (63 nm)/Ag (12 nm)/TiO_2 (63 nm)/Ag (12 nm)/TiO_2 (30 nm)/glass, SiN_x (51 nm)/Ag (12 nm)/SiN_x (89 nm)/Ag (12 nm)/SiN_x (75 nm)/Ag (12 nm)/SiN_x (75 nm)/Ag (12 nm)/SiN_x (36 nm)/glass.

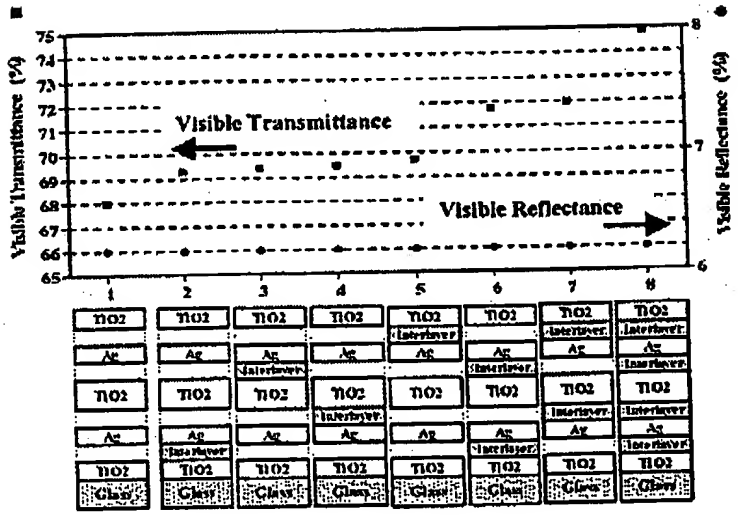

Fig. 3. Visible transmittance and visible reflectance of the Ag/TiO_2 stacks including two Ag layers (14 nm thick) with and without 1-nm-thick SiN_x interlayer(s). Squares and circles represent the visible transmittance and reflectance, respectively.

mittance by the ZnO insertion is almost the same as the SiN_x case.

The results given in Figs. 2 and 3 indicate that the absorption occurs at the interface between the silver layer and the dielectric-material layer and the absorption is larger in the case of the dielectric material having a higher dielectric constant.

3.2. XPS analysis of the surface plasmon of silver

In order to analyze the characteristics of surface related excitation in silver layer, we prepared the silver layers overcoated with thin dielectric material and made X-ray photoelectron spectroscopy (XPS) surface analysis, which offers the information on the interface between silver and dielectric layer.

Fig. 4 shows the XPS spectra around Ag 3d peaks of the silver layers overcoated with TiO_2 and the plasmon loss peaks were observed at the higher energy side of the Ag $3d_{5/2}$ (at 368 eV) and Ag $3d_{3/2}$ (at 374 eV) peaks [4]. Since Ag 3d peaks of the single silver layer and the TiO_2-overcoated silver layers are at the same position and also have almost the same shape, it is obvious that the silver overcoated with TiO_2 is not oxidized, which is confirmed by the results that there is no change in the electrical resistance of the silver layers

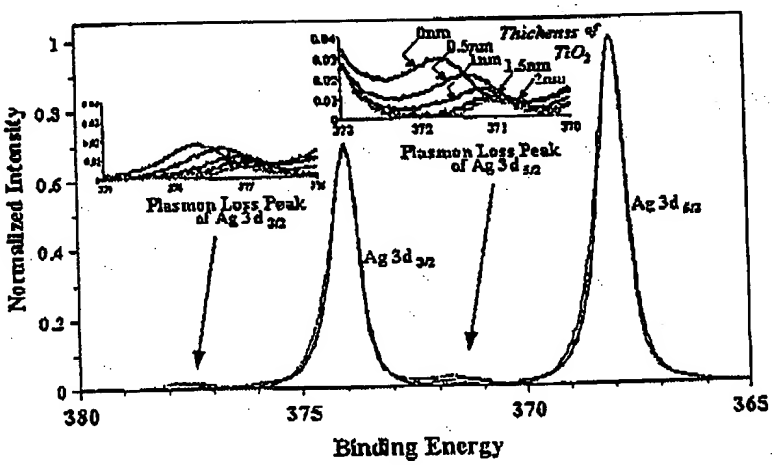

Fig. 4. The XPS spectra around the Ag $3d_{5/2}$ and Ag $3d_{3/2}$ peaks of the silver layers overcoated with TiO_2 layer having various thicknesses. Internal figures are the enlargements of the plasmon loss peaks.

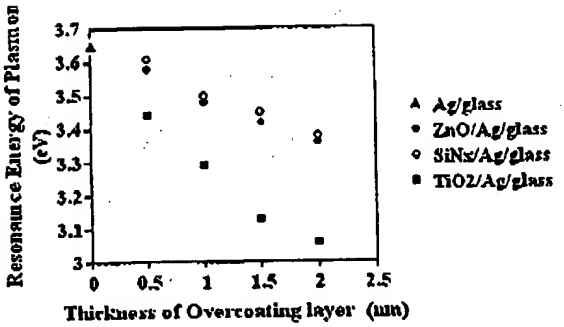

Fig. 5. The resonance energy of the surface plasmon of silver. Triangles represent that of silver monolayer. Circles painted and unpainted represent that of silvers overcoated with ZnO and SiN_x, respectively. Squares represent that of silvers overcoated with TiO_2.

by overcoating with TiO_2. It is also obvious that the plasmon loss peaks shift to the lower energy side with increasing the thickness of overcoated TiO_2, which means that the resonance energy of the surface plasmon, generated at the interface between silver and TiO_2, decreases with the TiO_2 thickness. We also investigated the silver layers overcoated with SiN_x and ZnO and obtained the same tendency on the surface plasmon.

In Fig. 5, the resonance energy of plasmon is plotted against the thickness of overcoated dieletric materials. It can be seen that the resonance energy of surface plasmon decreases with the increase of the dielectric-layer thickness and the resonance energy decreases more when the dielectric material has a higher dielectric constant.

These results can be explained by the equation for the resonance frequency of the surface plasmon [5]:

$$\omega_s = \omega_p/(\epsilon+1)^{1/2}, \quad (1)$$

$$\omega_p^2 = 4\pi ne^2/m^*, \quad (2)$$

where ω_s is the resonance frequency of the surface plasmon, ω_p is the resonance frequency of the bulk plasmon, ε is the dielectric constant of the dielectric material, n is the density of free electrons, e is charge of electron and m^* is the effective mass of electron.

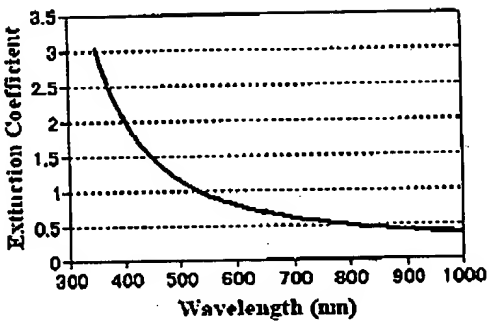

Fig. 7. Extinction coefficient of the absorbing layer.

The increase of the thickness of dielectric overlayers can be understood to increase the effective dielectric constant of dielectric material, which is denoted as ε in Eq. (1). In this case, namely the overlayer thickness is too small comparing with the extension of the electromagnetic field generated by the surface plasmon, the effective dielectric constant can be considered as a definite integral of the dielectric constants of dielectric material and vacuum by using a weight function corresponding to the electromagnetic field strength, as illustrated in Fig. 6. It can be explained from the increase of effective dielectric constant of the adjacent medium to the silver layer that the resonance energy of surface plasmon decreases with the thickness and/or the dielectric constant of the overlayer.

3.3. Ellipsometric analysis of the surface plasmon

For ellipsometric analysis, we prepared the stacks with a layer construction of Ag/TiO_2/glass. By considering the contribution of the surface plasmon, we employed the layer stack model of Ag/Absorbing layer/TiO_2/glass. The optical constants and the thickness of the absorbing layer were evaluated by the ellipsometric analysis with a good fitting to both of the measured transmittance and ellipsometric data. The obtained extinction coefficient of the absorbing layer is presented in Fig. 7. The obtained thickness of the absorbing layer is below 1 nm and does not raise the optical interference practically. The calculated transmittance considering this

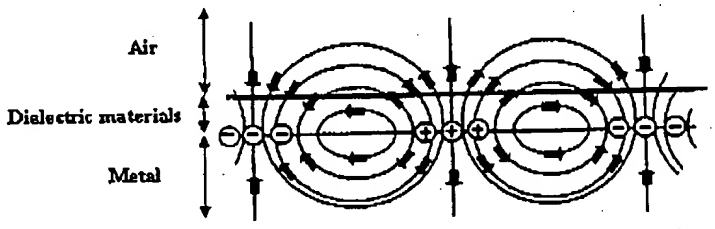

Fig. 6. Schematic diagram of the electromagnetic field generated by the surface plasmon excited around the interface between silver and dielectric material.

surface plasmon absorption agrees well with the measured transmittance and the calculated and measured reflectance are coincident well also.

4. Conclusion

We investigated the optical properties of the silver/dielectric-material multilayers and found that the absorption exists at the silver/dielectric-material interfaces. The absorption was assigned to the absorption of surface plasmon by spectral, ellipsometric and XPS analyses.

The absorption was detected as the difference between the measured transmittance and the calculated one. It is found that the absorption increases with the number of the silver/dielectric-material interfaces and with the dielectric constant of the dielectric materials. By considering the absorbing layer at the silver/dielectric-material interface, the ellipsometric analysis gives a good fit of the optical constants and thicknesses of constituent layers and the measured transmittance agrees well with the calculated one using the ellipsometrically obtained results.

The surface plasmon loss peaks of Ag $3d_{5/2}$ and Ag $3d_{3/2}$ were observed by the XPS analysis of the silver layer overcoated with the dielectric layers. The resonance energy of surface plasmon decreases with the increase of the dieletric-layer thickness and the resonance energy of surface plasmon decreases more when the dielectric material has a higher dielectric constant. This energy shift of the surface plasmon can be explained by using a well-known equation giving the resonance frequency of surface plasmon. These XPS results are consistent with the results on the spectral analysis and ellipsometric analysis.

We also found that the transmittance of the silver/dielectric-material multilayers can be increased by inserting the thin interlayers having a low dielectric constant into the silver/dielectric-material interfaces; this method is especially effective in obtaining the high performance Ag/TiO_2 multilayers.

Acknowledgments

The authors are grateful to J.A. Woollam Japan Corp. for their technical assistance.

References

[1] H. Ohsaki, Y. Tachibana, Thin Solid Films, in press.
[2] H. Ohsaki, Y. Tachibana, K. Moriwaki, Properties of Antireflective Coatings and its Design and Production Technologies, Gijyutu-Joho-Kyokai, Tokyo, 2001, p. 184, in Japanese.
[3] Y. Tachibana, H. Ohsaki, A. Hayashi, A. Mitsui, Y. Hayashi, Vacuum 59 (2000) 836.
[4] C.W. Bates Jr., G.K. Wertheim, D.N.E. Buchanan, Phys. Lett. Part A 72 (1979) 178.
[5] R.H. Ritchie, Phys. Rev. 106 (1957) 874.

ELSEVIER

Thin Solid Films 351 (1999) 57–60

thin solid films

High rate sputter deposition of TiO_2 from TiO_{2-x} target

Hisashi Ohsaki*, Yuko Tachibana, Atsushi Hayashi, Akira Mitsui, Yasuo Hayashi

Research Center, Asahi Glass Co. Ltd., Hazawa-cho, Kanagawa-ku, Yokohama 221-8755, Japan

Abstract

A new sputter technique for high rate deposition of TiO_2 was developed for applying to common planar magnetron sputter system. With this technique, using plasma sprayed TiO_{2-x} targets and a sputter gas of a few percent of O_2 diluted with Ar, TiO_2 films are deposited with a high deposition rate efficiency (deposition rate per applied power density) being almost eight times larger than that of the conventional sputter method using Ti target and O_2 sputter gas. © 1999 Elsevier Science S.A. All rights reserved.

Keywords: Sputtering; Titanium oxide

1. Introduction

Demand for optical coatings on large area substrates for architectural, automotive and display applications as well as on small area coating for optical components which already have a very long history of vacuum vapor deposition is increasing. Because sputter method leads to high uniformity on thickness and film quality, the sputter deposition has been becoming a mainstream for the large area coating. The principal materials used for optical layers are low-refractive-index and high-refractive-index materials like as SiO_2 and TiO_2, respectively. Stable sputter deposition of SiO_2 has been established recently by new technologies for diminishing the arcing problems: rotateable cylindrical magnetron [1], mid-frequency AC dual magnetron sputtering [2,3] and pulse modulation DC sputtering [4,5]. On the other hand, TiO_2 sputter deposition has a low deposition rate problem when the conventional sputtering method are used and its deposition rate has been improved by controlling the metal mode by measuring the plasma emission [6] and by using mid-frequency AC dual magnetron system [7]. Those high rate sputter techniques for depositing TiO_2 films unfortunately need some special components: plasma emission monitor and O_2 inflow feedback system for the former technique or dual magnetron system and O_2 partial pressure monitor for the latter.

We have developed a simple TiO_2 high rate sputter method which does not need any special cathode, uncommon power supply or feedback system and which uses only a TiO_{2-x} target instead of a Ti metal target. In this paper, we will describe the mechanism of this high rate sputter method.

2. Experimental

We used in-line type planar magnetron sputter machines (Nisshin Seiki Co., JVS-S0-3 and BOC Coating Technology, ILS-1600) having a deposition chamber with a load lock and over run chambers on both ends. The deposition chamber is divided into three chambers with one cathode in each one. The sputter gas is introduced to each deposition chamber and evacuated through the end chambers with two diffusion pumps. The DC power supply is a switching regulator (Advanced Energy Ind., MDX), which can be controlled within voltage, current and power regulation modes; power regulation mode was selected.

Films were deposited on soda-lime glass plates and Au sheets. The thickness of the films was measured using a stylus-type surface tracer (Rank Taylor Hobson, Talystep). The deposition rate was evaluated by dividing the film thickness by the passage time of the substrate through the deposition chamber. The refractive index of the films was analyzed by ellipsometry using a spectroscopic ellipsometer (J.A. Woollam Co., Inc , VASE) and the extinction coefficient of films were evaluated from the visible transmittance and reflectance using a grating-type spectrometer (JASCO, ART-25GT). The depth profiles of the films were obtained using an X-ray photoelectron spectroscope (Physical Electronics, Quantum 2000).

Negative ion implantation into films and transmittance through films were calculated using a Monte Carlo program, TRIM [8] and the results were used for analyzing the species

* Corresponding author. Tel.: +81-45-374-8758; fax: +81-45-374-8852.

E-mail address: ohsaki@agc.co.jp (H. Ohsaki)

0040-6090/99/$ - see front matter
PII: S0040-6090(99)00207-2

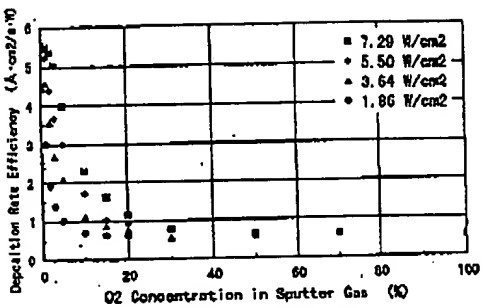

Fig. 1. Deposition rate efficiency vs. O_2 concentration in sputter gas and power density for sputtering of TiO_{2-x} target. Expected error of O_2 concentration is less than ±2% and that of deposition rate efficiency is less than ±5%.

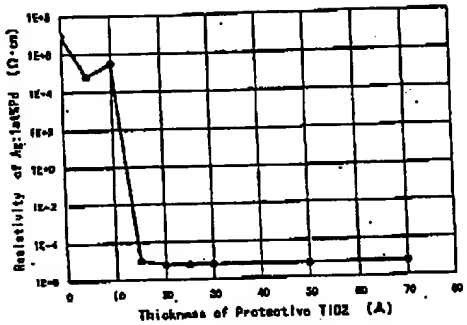

Fig. 3. Resistivity of Ag:1 at.% Pd films protected by TiO_2 films (TiO_{2-x}: 3% O_2) with various thicknesses after additional sputter deposition of TiO_2(Ti-100% O_2). Expected error of resistivity is a few percent. Line is drawn as guides for the eyes.

reaching onto the film surface by comparing the experimentally obtained depth profiles of the deposited films.

3. Results and discussion

3.1. Sputtering mechanism of TiO_{2-x}

TiO_2 target was produced by plasma spray of TiO_2 powder and the obtained material was a n-type semiconductor having a sufficient conductivity of ca. 0.3 Ω · cm as a target for DC sputtering. Films were deposited on glass substrates by sputtering the TiO_{2-x} target with gas mixtures of Ar and O_2. The deposition rate efficiency (deposition rate per applied power density) is plotted with various power densities in Fig. 1. The deposition rate efficiency becomes large when using a sputtering gas including less O_2 and larger applied power.

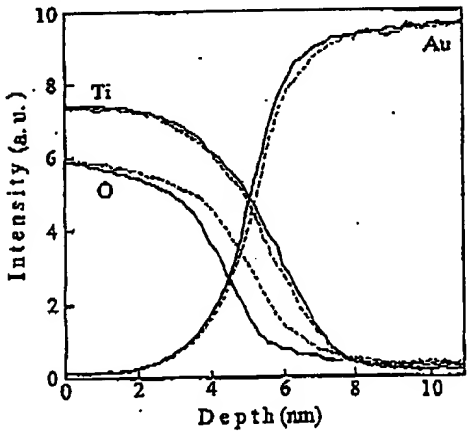

Fig. 2. XPS depth profiles of sputter-deposited TiO_2 on Au substrate. Solid lines are in TiO_{2-x} target-3% O_2/Ar sputtering case and dashed lines are in Ti target-100% O_2 case.

It is known that the deposition rate efficiency strongly depends on the surface state of the target and the efficiency increases when the target surface becomes more metallic [4,9,10]. The surface state of the TiO_{2-x} target bombarded with Ar ions was measured by X-ray photoelectron spectroscopy (XPS) and it was found that the bombarded surface changes to metal rich comparing to the original surface. From this result, the surface state of the TiO_2 target during the sputtering can be said to be rather metallic. The deposition rate efficiency of Ar sputtering of Ti metal target is about 7.5 Å · cm^2/s · W and the efficiency of fully oxidized Ti target (sputtered with 100% O_2 sputter gas) is 0.37 Å · cm^2/s · W. Therefore, the target surface of sputtered TiO_{2-x} with Ar is not purely metallic (the deposition rate efficiency being 5.5 Å · cm^2/s · W, as shown in Fig. 1) but has a certain degree of oxidation. The target surface of TiO_2 sputtered with an Ar-O_2 sputter gas reaches a certain surface steady state which is more oxidized compared to pure Ar sputtering case. This surface state discrepancy between Ar-O_2 and Ar sputtered TiO_{2-x} target increases with an increase of O_2 concentration and with a decrease of applied power. This tendency is reasonable considering that Ar bombardment makes the surface metal-rich, O_2 bombardment oxidizes the surface and the sputtering yield of O_2 ions is about 0.4 times smaller than that of Ar ions. This sputtering yield ratio was obtained from the experimental results on the sputtering of Au target using Ar and O_2 sputter gases.

3.2. Ejected species from TiO_{2-x} target

For making clear that the ejected O-related species from TiO_{2-x} target reach directly the substrate or mix into the sputter gas, we estimated the kinetic energy of the O-related species by measuring the depth profiles of O atoms penetrating into the substrate. TiO_2 films were deposited on Au

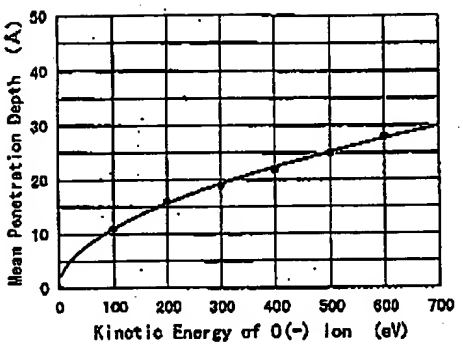

Fig. 4. Mean penetration depth of implanted O^- ions into Ag film. Line is a least-square-fitted relationship between mean penetration depth (d) and kinetic energy (E), $d = E^{0.51}$.

sheets for avoiding the chemical reaction between deposited species and substrate and the deposition was done by the ways: sputtering of a TiO_{2-x} target with 3% O_2 gas and sputtering of a Ti target with 100% O_2 gas. XPS depth profiles in and around the interface of TiO_2 film/Au substrate were measured and are presented in Fig. 2. It shows that O species penetrates into Au about 10 Å deeper in the case of Ti-100% O_2 sputtering than in the case of TiO_{2-x}-3% O_2 sputtering.

It was also found that TiO_{2-x}-3% O_2 sputtering makes no damage on easily deterioratable material, as for example Ag deposited just before this TiO_2 deposition. This TiO_2 deposited by TiO_{2-x}-3% O_2 sputtering was used as a protective layer and the kinetic energy of O-related species coming from the O_2 sputtering gas was evaluated. TiO_2 films were deposited by Ti-100% O_2 sputtering on this protective TiO_2/Ag:1 at.% Pd/glass and the resistivity of Ag:1 at.% Pd was

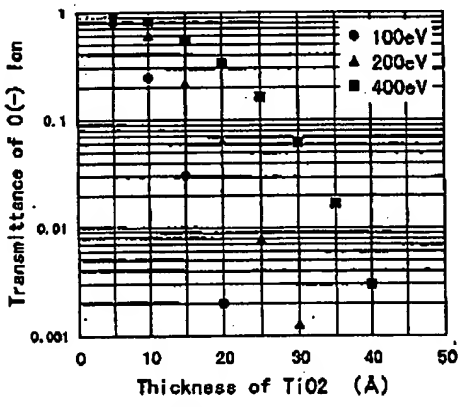

Fig. 5. Transmittance of O^- ions with various kinetic energies through TiO_2 film.

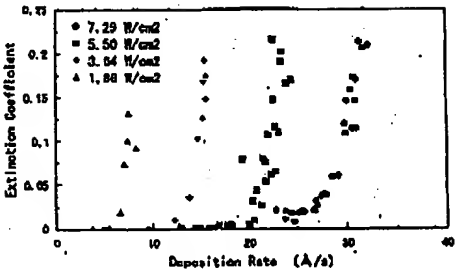

Fig. 6. Extinction coefficient of the films deposited from TiO_{2-x} target vs. deposition rate. Expected error of extinction coefficient is about ±10%.

measured (Fig. 3). Fig. 3 shows that O species are implanted into the substrate in a 10 Å depth at least during Ti-100% O_2 sputtering.

The upper two results are consistent with each other and it can be said that O_2 sputter gas is decomposed and changed to O^- ions in the plasma and then the O^- ions accelerated by the electric field around the target reaches the deposited film. In the case of TiO_{2-x} sputtering, O species ejected from the target do not mix in the sputter gas and reach the deposited film surface with a small kinetic energy.

The mean penetration depth of implanted O^- ions into Ag film was calculated by using the TRIM Monte Carlo program [8] and the results are presented in Fig. 4; an almost identical relationship between mean penetration depth and kinetic energy was also obtained in the case of O^- implantation into Au. This result indicates that the O species from TiO_{2-x} target has a kinetic energy of a few tens of eV. Fig. 5 shows the calculated transmittance of O^- ions with various kinetic energies through TiO_2. From Fig. 4 and Fig. 5, O^- ions from O_2 sputter gas is thought to have a kinetic energy of several hundreds of eV.

3.3. Formation mechanism of films

As mentioned above, Ti- and O-related species ejected from TiO_{2-x} target reach the substrate surface with rather

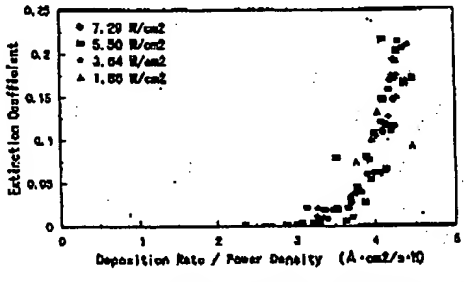

Fig. 7. Extinction coefficient of the films deposited from TiO_{2-x} target vs. deposition rate efficiency (deposition rate per applied power density). Expected error of extinction coefficient is about ±10%.

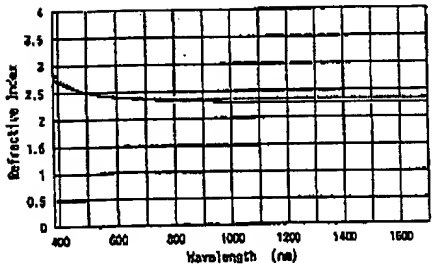

Fig. 8. Refractive indexes of TiO_2 films evaluated by ellipsometric analysis. TiO_2 films were obtained by 3% O_2 sputtering of TiO_{2-x} target (solid line) and 100% O_2 sputtering of Ti target (dashed line). Applied power density was 7.29 W/cm^2 in both cases.

low energies but oxygen must be supplied from the sputter gas for filling up the oxygen lack in order to obtain TiO_2 films.

Fig. 6 shows the relationship between deposition rate and extinction coefficient of deposited films using sputter gases with various O_2 concentrations. If the oxygen is supplied thermally from the sputter gas, the films deposited with low deposition rate have low extinction coefficient but, as Fig. 6 indicates, the amount of thermal oxygen is not large enough to fill up the oxygen lack even in the lower deposition rate case. On the other hand, Fig. 7 shows that the amount of filling-up oxygen is proportional to the applied power density. This means that the filling-up oxygen may be an excited oxygen and its amount is in proportion to the applied power density.

Transparent TiO_2 were obtained with about 8–9 times higher deposition rate by TiO_{2-x} sputter comparing with Ti-100% O_2 sputter and the measured refractive index of both films are almost the same as shown in Fig. 8.

4. Conclusion

A new sputter method for high rate deposition of TiO_2 was developed and applied to a common planar magnetron sputter system. In this technique, TiO_2 films are deposited by using plasma sprayed TiO_{2-x} targets and a sputter gas of a few percent of O_2 diluted in Ar. The deposition rate efficiency is almost eight times larger than that of the conventional sputter method using Ti target and O_2 sputter gas.

The XPS analysis showed that the surface of Ar-bombarded TiO_{2-x} becomes Ti rich suggesting that the high deposition rate efficiency of this new method comes from the metallic surface of the target during the sputtering.

From the results of XPS measurements analyzing the O implantation depth in a Au substrate and a Monte Carlo simulation, the O reluted species sputtered from the TiO_{2-x} target reach the deposited film surface with several tens of eV. Therefore, the released O is thought to be only slightly miscible with the sputter gas and negligible amount of O negative ions are generated. This TiO_{2-x} sputtering does not make heavy damages on the easily deterioratable materials, as for example Ag deposited just before a TiO_{2-x} deposition.

Oxygen is supplied from the sputter gas to fill up the oxygen lack of deposited film during the TiO_{2-x} sputtering and transparent TiO_2 is obtained. The supplied oxygen is thought to be in an excited state and its amount is proportional to applied power density. Transparent TiO_2 films were obtained with about 8–9 times higher deposition rate using TiO_{2-x} sputtering compared to Ti-100% O_2 sputtering. TiO_2 films prepared by both methods have almost the same refractive index.

Acknowledgements

The authors are grateful to Mr K. Kadowaki and Mr K. Sasuki for technical assistance.

References

[1] A. Belkind, W. Gerristead Jr., Z. Orban, Thin Solid Films 207 (1992) 319.
[2] S. Schiller, V. Kirchhoff, T. Kopte, Proc. 3rd Int. Symp.: Sputtering Plasma Processes, 1995 p. 71.
[3] G. Bräuer, J. Szczyrbowski, G. Teschner, J. Non-Cryst. Solids 218 (1997) 19.
[4] H. Ohsaki, Y. Tachibana, J. Shimizu, T. Oyama, Thin Solid Films 281-282 (1996) 213.
[5] R.A. Scholl, Soc. Vacuum Coater 36th Ann. Technol. Conf. Proc., 1993a p. 405.
[6] S. Schiller, O. Heisig, Chr. Korndörfer, G. Beister, J. Reschke, K. Steinfelder, J. Strümpfel, Surf. Coat Technol. 33 (1987) 405.
[7] J. Szczyrbowski, G. Bräuer, G. Teschner, A. Zmelty, J. Non-Cryst. Solids 218 (1997) 25.
[8] J.P. Ziegler, J.P. Biersack, The Stopping and Range of Ions in Solids, Pergamon Press, New York, 1985.
[9] H. Ohsaki, Proc. 3rd Int. Symp.: Sputtering and Plasma Processes, 1995, p. 241.
[10] H. Ohsaki, Thin Solid Films 281-282 (1996) 223.